

Original Article

# Effects of *Siraitia grosvenorii* extract on nonalcoholic steatohepatitis-like lesions in Sprague Dawley rats fed a choline-deficient, methionine-lowered, L-amino acid-defined diet

Kinuko Uno<sup>1</sup>, Katsuhiro Miyajima<sup>2\*</sup>, Shuji Ogawa<sup>1</sup>, Noriko Suzuki-Kemuriyama<sup>2</sup>, and Dai Nakae<sup>2,3</sup>

<sup>1</sup> Department of Food and Nutritional Science, Graduate School of Agriculture, Tokyo University of Agriculture, 1-1-1 Sakura-ga-Oka, Setagaya, Tokyo 156-8502, Japan

<sup>2</sup> Department of Nutritional Science and Food Safety, Faculty of Applied Biosciences, Tokyo University of Agriculture, 1-1-1 Sakura-ga-Oka, Setagaya, Tokyo 156-8502, Japan

<sup>3</sup> Department of Medical Sports, Faculty of Health Care and Medical Sports, Teikyo Heisei University, 4-1 Uruido-Minami, Ichihara, Chiba 290-0193, Japan

**Abstract:** *Siraitia grosvenorii* is the fruit of a cucurbitaceous vine endemic to China. Its extract has been used as a sweetener and exhibits various anti-inflammatory and anticarcinogenic effects mediated via its antioxidant properties. In the present study, we aimed to clarify the preventive or ameliorative effects of *S. grosvenorii* extract (SGE) on nonalcoholic steatohepatitis-like lesions induced in male Hsd: Sprague Dawley rats fed a choline-deficient, methionine-lowered, L-amino acid-defined diet for 13 weeks. This diet increased hepatotoxicity parameters and upregulated the expression of inflammation- and fibrosis-related genes in the liver, resulting in the progression of hepatic lesions, oxidative stress, hepatocellular apoptosis, and fibrosis. Furthermore, this diet upregulated the expression of phosphorylated nuclear factor- $\kappa$ B (NF- $\kappa$ B) and CD44. SGE administration inhibited these lesions, similar to CD44, a factor that controls hepatic inflammation and fibrosis. These results revealed that SGE impacts the disease stage via antioxidative effects and regulation of CD44 expression. SGE was found to be useful for preventing and treating steatohepatitis. (DOI: 10.1293/tox.2022-0043; J Toxicol Pathol 2023; 36: 1–10)

**Key words:** nonalcoholic steatohepatitis, fibrosis, *Siraitia grosvenorii*, oxidative stress, NF-kappa B, CD44

## Introduction

Lifestyle-related diseases are associated with lifestyle habits such as diet, lack of exercise, alcohol consumption, and smoking, and the suppression of such diseases has become an urgent issue in recent years. Therefore, optimal strategies for disease control must be developed by identifying underlying mechanisms and key factors impacting the disease. Some foods and their components have been reported as regulatory factors in metabolic syndromes<sup>1–3</sup>. Nonalcoholic fatty liver disease (NAFLD) is a liver phenotype, occasionally progressing to nonalcoholic steatohepatitis (NASH) with inflammation and fibrosis, and subsequently cirrhosis and hepatocellular carcinoma<sup>4</sup>. Liver disease-re-

lated mortality is known to increase with the progression of liver fibrosis<sup>5</sup>; however, definitive therapy for severe liver fibrosis is yet to be established, and the only known effective treatment for cirrhosis is liver transplantation.

The underlying mechanisms of NAFLD/NASH have been investigated in basic research using various animal models and clinical studies. The choline-deficient, methionine-lowered, L-amino acid-defined (CDAA) diet has been established as a major NASH model in male rats. However, this animal model fails to adequately simulate human NASH in terms of disturbed very low-density lipoprotein production, body weight changes, and insulin resistance, although similarities, especially considering oxidative stress and hepatic fibrosis, should be noted<sup>6–8</sup>. Importantly, this dietary model can be induced by nutritional modification without harmful or carcinogenic chemicals or genetically modified animals.

*Siraitia grosvenorii* fruit is well-known for its sweet taste, and its extract is widely employed as a sweetener and in edible traditional medicine to treat pharyngitis and pharyngeal pain, as well as an anti-tussive remedy in China<sup>9</sup>. *S. grosvenorii* comprises mogrosides, particularly mogroside V. Owing to its molecular structure, mogroside V is 200–350 times sweeter than sucrose and possesses antioxidant,

Received: 4 April 2022, Accepted: 16 August 2022

Published online in J-STAGE: 9 September 2022

\*Corresponding authors: K Miyajima

(e-mail: km206186@nodai.ac.jp);

D Nakae (e-mail: agalennde.dai@nifty.com; d.nakae@thu.ac.jp)

©2023 The Japanese Society of Toxicologic Pathology

This is an open-access article distributed under the terms of the Creative Commons Attribution Non-Commercial No Derivatives

(by-nc-nd) License. (CC-BY-NC-ND 4.0: <https://creativecommons.org/licenses/by-nc-nd/4.0/>).



hypoglycemic, blood lipid-depressing, anti-inflammatory, and anticarcinogenic activities<sup>10</sup>.

Reportedly, *S. grosvenorii* can prevent hepatic steatosis in a NAFLD mouse model fed a high-fat diet<sup>11, 12</sup>. In NASH model mice fed a CDAA high-fat diet without trans fatty acids, *S. grosvenorii* could inhibit the progression of inflammation and fibrosis<sup>13</sup>. However, the mechanisms underlying these actions and their associated factors remain unclear. Herein, we examined the effects of sweeteners on the pathogenesis and underlying mechanisms of lifestyle-related diseases in animal models. A NASH rat model fed a CDAA diet was used to examine disease suppression mediated by *S. grosvenorii* extract (SGE).

## Material and Methods

### Test compounds

SGE was provided by San-Ei Gen F.F.I. Inc. (Osaka, Japan) and administered in distilled drinking water for 13 weeks at concentrations of 0.06, 0.2, and 0.6% (w/v). The SGE water samples were prepared five days a week. These concentrations were selected based on previous studies<sup>13–15</sup>. The no-observed-adverse-effect level of SGE was  $\geq 5\%$  in Wistar Hannover rats<sup>16</sup>. A preliminary study was conducted using solutions of 0.06, 0.2, 0.6, 2.0, and 6.0% SGE in drinking water; water consumption decreased by more than 2.0% (data not shown). This SGE comprised more than 50% mogroside V (Table 1).

### Antioxidant activity assay

The antioxidative effect of SGE (100 mg/mL, 50% ethanol) was evaluated using the 1,1-diphenyl-2-picrylhydrazyl (DPPH) assay according to the standard method. The calculated Trolox equivalent value per sample was 1 mg, and these sample values were determined in duplicate. L (+)-ascorbic acid (0.030 mg/mL, 50% ethanol, FUJIFILM Wako Pure Chemical Corporation, Osaka, Japan) and d-alpha-tocopherol (0.139 mg/mL, 50% ethanol, Combi-Blocks, Inc., San Diego, CA, USA) were used as positive controls for antioxidants, and mogroside V (50 mg/mL 50% ethanol, FUJIFILM Wako Pure Chemical Corporation) was examined as the active substance in SGE. The mogroside V dose was determined based on SGE content (Table 1).

**Table 1.** SGE Nutrient Composition

Nutrient (%)	SGE
Protein	8.2
Fat	0
Carbohydrate	86.9
Dietary fiber	0
Ash	0.2
Moisture	4.7
Total	100
Mogroside V	58.4

SGE: *Siraitia grosvenorii* extract.

### Animals and treatments

In total, male Hsd: Sprague Dawley (SD) rats (5 weeks of age) were purchased from SLC Inc. (Shizuoka, Japan) and housed at an average temperature of 23°C under air-controlled conditions in colony cages with a 12 h light/12 h dark cycle. The rats were fed a basal diet (CE-2; CLEA Japan Inc., Tokyo, Japan) and tap water *ad libitum* during the acclimation period. At six weeks of age, the rats were divided into six equal groups based on their body weights (n=6, shown in Table 2). The control and SGE groups received a standard diet (CE-2), whereas other groups were fed a CDAA diet (A1603203, choline 0%, methionine 0.17%, fat 15%, and 30 kcal%; Research Diets Inc., New Brunswick, NJ, USA) for 13 weeks. Body weights and food intake were monitored weekly. SGE was prepared five days per week. As no significant changes in water intake were observed during the preliminary study, the water consumption was monitored weekly.

After the feeding period, the rats were fasted overnight and dissected under isoflurane anesthesia. Blood was sampled from the abdominal aorta to obtain serum samples for biochemical examinations. The rats were euthanized by exsanguination under isoflurane anesthesia. During necropsy, the livers were excised and weighed; some specimens were immediately fixed in 10% neutral buffered formalin for histopathological and immunohistochemical examinations, and the remaining liver samples were stored at -80°C for molecular biological assessments.

### Serum biochemical examinations

Serum alanine aminotransferase (ALT) and aspartate aminotransferase (AST) levels were measured using a transaminase CII-test kit (Wako Pure Chemical Corporation).

### Molecular biological examinations

Total hepatic RNA was extracted using Sepasol-RNA (Nacalai Tesque, Inc., Kyoto, Japan) and reverse-transcribed to cDNA using PrimeScript RT Master Mix (Takara Bio Inc., Shiga, Japan) and TaKaRa PCR Thermal Cycler Dice Touch (Takara Bio Inc.). After the reaction, cDNA samples were diluted five times with sterile water and subjected to reverse transcription-quantitative PCR (RT-qPCR) using TB Green Premix Ex Taq II (Takara Bio Inc.) and a Thermal Cycler Dice Real Time System II (Takara Bio Inc.). The

**Table 2.** Experimental Groups

Group	Drink	Diet
Control	distilled water	basal diet
SGE	SGE, 0.6%	
CDAA	distilled water	CDAA diet
SGE 0.06%/ CDAA	SGE, 0.06%	
SGE 0.2%/ CDAA	SGE, 0.2%	
SGE 0.6%/ CDAA	SGE, 0.6%	

SGE: *Siraitia grosvenorii* extract; CDAA: choline-deficient, methionine-lowered, L-amino acid.

samples were amplified using TB Green Premix Ex Taq II (Takara Bio, Inc.). All procedures were performed in accordance with the manufacturer's protocol. The fold-changes in gene expression relative to the levels obtained in the control group, which were set to 1, were analyzed and calculated using the  $2^{-\Delta\Delta C_t}$  method. Primer sequences used for qPCR are listed in Table 3.

### Western blot analysis

Hepatic total protein was extracted using traditional methods, and the protein concentration was measured using the Protein Assay BCA kit (Nacalai Tesque Inc.). Protein samples from each animal were pooled for each group, separated by sodium dodecyl sulfate-polyacrylamide gel electrophoresis (SDS-PAGE), and transferred to polyvinylidene fluoride (PVDF) membranes. These protocols were performed by Bio-Rad Laboratories, Inc. (Tokyo, Japan). After blocking with 5% skim milk, the membranes were incubated with primary antibodies against NF-kappa-B (1:1,000, Cell Signaling Technology, Danvers, MA, USA), phospho-NF- $\kappa$ B (1:1,000; Cell Signaling Technology), and glyceraldehyde-3-phosphate dehydrogenase (GAPDH, 1:3,000; Santa Cruz Biotechnology, Inc., Dallas, TX, USA). Anti-rabbit IgG, HRP-linked antibodies (Cell Signaling Technology), and anti-mouse IgG (Cell Signaling Technology) were used as secondary antibodies, and signals were visualized using the Clarity Max™ Western ECL Substrate IgG, HRP-linked Antibody (Bio-Rad Laboratories, Inc.) and detected using the Bio-Rad ChemiDoc™ Touch Imaging System (Bio-Rad Laboratories, Inc.). These proteins were analyzed using ImageJ (National Institutes of Health, Bethesda, MD, USA).

### Histopathological examinations

The fixed livers were embedded in paraffin according to standard techniques and cut into 4- $\mu$ m sections for hematoxylin and eosin (H&E) and Sirius Red (SR) staining. In addition, immunohistochemical staining was performed using antibodies against CD44 (1:100; Cell Signaling Technology Inc.), CD68 (1:100; Abcam plc., Tokyo, Japan), and the glutathione *S*-transferase placental form (GST-P; 1:100; Medical & Biological Laboratories Co., Ltd., Aichi, Japan). Histofine Simple Stain Rat MAX-PO (MULTI) (Nichirei Bioscience

Inc., Tokyo, Japan) was used as the secondary antibody, and signals were visualized using 3,3'-diaminobenzidine (Wako Pure Chemical Industries, Ltd., Osaka, Japan). TdT-mediated dUTP nick end labeling (TUNEL) (ApopTag Plus Peroxidase *In Situ* Apoptosis Detection Kit; EMD Millipore Corporation, Billerica, MA, USA) was performed to detect hepatocellular apoptosis, according to the manufacturer's protocol. Using SR-stained specimens, fibrotic areas were measured using CellSens Dimension software (Olympus Life Science Solutions, Tokyo, Japan). For GST-P immunohistochemical staining, the positive foci area (>1,000  $\mu$ m<sup>2</sup>) was measured using ImageJ software, and the rate of positive area in the liver section was calculated as aggregation by the group. CD68 immunohistochemical staining was graded from normal (−) to severe (3+). Grade ( $\pm$ ) was used to represent very weakly positive changes, (+) to represent focal or weakly positive sections, (2+) to indicate half of the section area with positive or moderate changes, and (3+) to indicate more than half of the whole area with positive or severe changes in a tissue section. CD44 immunohistochemical staining was performed on positive bile ducts (>80% cells in the bile duct) per total bile duct.

### Statistical analysis

Data values are expressed as the mean  $\pm$  standard deviation. Statistical analyses were performed using GraphPad Prism ver. 6.05 (GraphPad Software, San Diego, CA, USA). The significance of differences between groups was examined using one-way analysis of variance (ANOVA) and Tukey's multiple comparison test. Statistical significance was set at  $p < 0.05$ .

## Results

### Antioxidant activity assay

The changes in antioxidative values are shown in Fig. 1. The antioxidant activities of SGE and mogroside V were constant. The free radical scavenging rate for SGE and mogroside V were 49.5 and 21.9%, respectively. Accordingly, mogroside V could play a role in mediating the antioxidative effect of SGE.

**Table 3.** Gene-specific Primers

Gene	Forward primer	Reverse primer
Gpx2	GAGGAACAACACTACCCGGGAC	GGAAGCCGAGAACCCT
MCP-1	CTTCCTCCACCACTATGCAGG	GATGCTACAGGCAGCAACTG
TNF-alpha	GAAGCTCAGCGAGGACACCAA	GCCAGTGTGTGAGAGGGACG
Collagen type 1	GTACATCAGCCCAAACCCCA	CAGGATCGGAACCTTCGCTT
Collagen type 4	CTTCGTTGGCCTCTGTTTGC	TGCACTGGATTGCAAAGGGC
TGF-beta	CCATGACATGAACCGACCCT	CTGCCGTACACAGCAGTTCT
CD44	TACTGGAGACCGGGATGACG	TGTTTCTGAGCTGTTGCTGG
GAPDH	AGTGCCAGCCTCGTCTCATA	AAGAGAAGGCAGCCCTGGTA

Gpx2: glutathione peroxidase 2; MCP1: monocyte chemotactic protein-1; TNF-alpha: tumor necrosis factor-alpha; TGF beta: transforming growth factor-beta; GAPDH: glyceraldehyde-3-phosphate dehydrogenase.

### Water intake and body and liver weight

Changes in body and liver weight and water intake are shown in Fig. 2. Although body weights sequentially increased in the control and SGE groups, those in the CDAA diet groups were lower than those in the control groups from week 2 to week 10 (Fig. 2A). Water intake tended to increase with increasing SGE concentrations (Fig. 2B). In addition, liver weights in the CDAA diet groups were greater than those in the control diet groups. In contrast, these weights decreased after administering 0.2% SGE (Fig. 2C and 2D).

### Serum biochemical examination

Changes in serum biochemical parameters are shown in Fig. 3. The CDAA diet groups showed increased AST and ALT activities. Administration of 0.2% and 0.6% SGE tended to decrease the AST value (Fig. 3A), and the ALT value decreased in SGE-treated groups (Fig. 3B).

### Molecular biological examination

Figure 4 presents changes in hepatic gene expression. The CDAA diet increased mRNA expression levels of monocyte chemoattractant protein-1 (Mcp-1), tumor necrosis factor-alpha (TNF-alpha), and glutathione peroxidase 2 (Gpx2), and administration of 0.2% SGE decreased these expression levels. The mRNA expression of transforming growth factor-beta (Tgf $\beta$ ) was upregulated by the CDAA diet and downregulated following the administration of 0.2% and 0.6% SGE. Similarly, the mRNA expression of collagen type 1, collagen type 4, and CD44 was elevated in the CDAA diet groups and reduced by 0.2% and 0.6% SGE.

### Western blot analysis

Alterations in hepatic protein expression are shown in Fig. 5. The CDAA diet increased the phosphorylation ratio of NF- $\kappa$ B, which decreased after SGE administration exceeding 0.2%.

### Histopathological examination

Morphological changes in the liver are shown in Fig. 6. The CDAA diet could induce NASH lesions, including fatty

changes in hepatocytes (Fig. 6B), CD68-positive macrophage infiltration (Fig. 6H), precancerous lesions such as GST-P-positive cell/foci (Fig. 6P), and fibrosis (Fig. 6E). Likewise, the CDAA diet-fed rats showed increased apoptosis of TUNEL-positive hepatocytes and elevated CD44-positive cells in the bile ducts (Fig. 6K). Conversely, there were no changes in the SGE group.

SGE administration ameliorated hepatic lesions, except for fatty changes in the hepatocytes. The CD68-positive macrophage infiltration score ranged between 2+ to 3+ in the CDAA group. In the 0.06% SGE group, the score was almost 2+, and treatment with 0.2 and 0.6% SGE decreased this score from + to 2+, which was more pronounced than that at 0.2% (Fig. 6I, Table 4). The number of apoptotic hepatocytes was decreased at all SGE concentrations (Fig. 6L). The area of SR-positive fibrosis (Fig. 6F) and percentage of CD44-positive cells in the bile ducts also decreased following treatment with 0.2 and 0.6% SGE (Fig. 6O). In precancerous GST-P-positive foci, medium foci were observed in the CDAA group, small-to large-sized foci were observed in the 0.06% SGE group (Fig. 6Q), and small foci were detected in the 0.2 and 0.6% SGE groups (Fig. 6R). Administration of 0.2 and 0.6% SGE tended to decrease after GST-P-positive foci (Table 5). GST-P-positive hepatocytes were sporadically detected in both foci and single cells in the CDAA group; SGE administration tended to decrease the presence of these cells.

## Discussion

NASH is a lifestyle-related disease with a risk of progressing to cirrhosis and hepatocellular carcinoma, and implementing prevention and treatment strategies remains critical to afford optimal control. In the present study, SGE and mogroside V demonstrated antioxidant effects. However, in addition to mogroside V, *S. grosvenorii* comprises various bioactive components<sup>17</sup>, and the contribution of these components should be considered. Thus, the antioxidant activity of SGE can be partly attributed to mogroside V, and other components may have contributed to this effect.

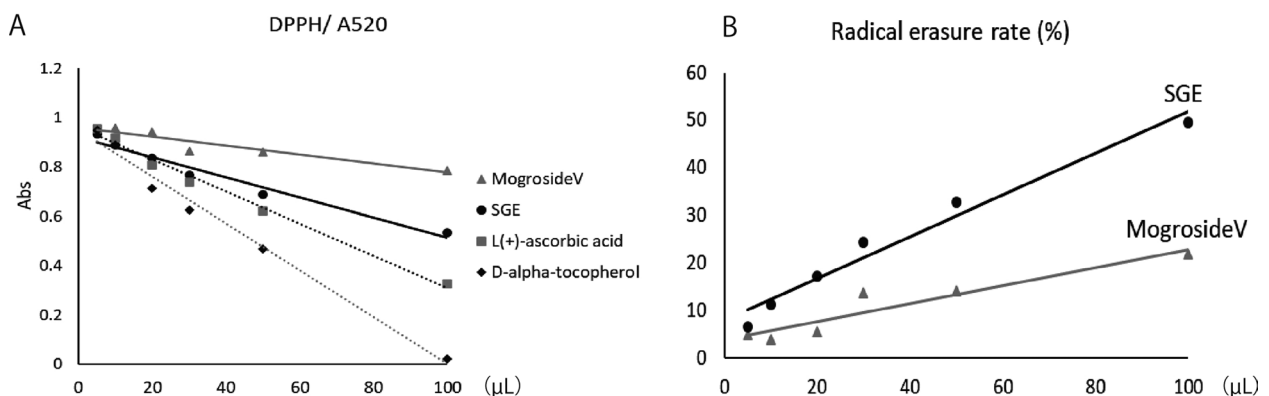
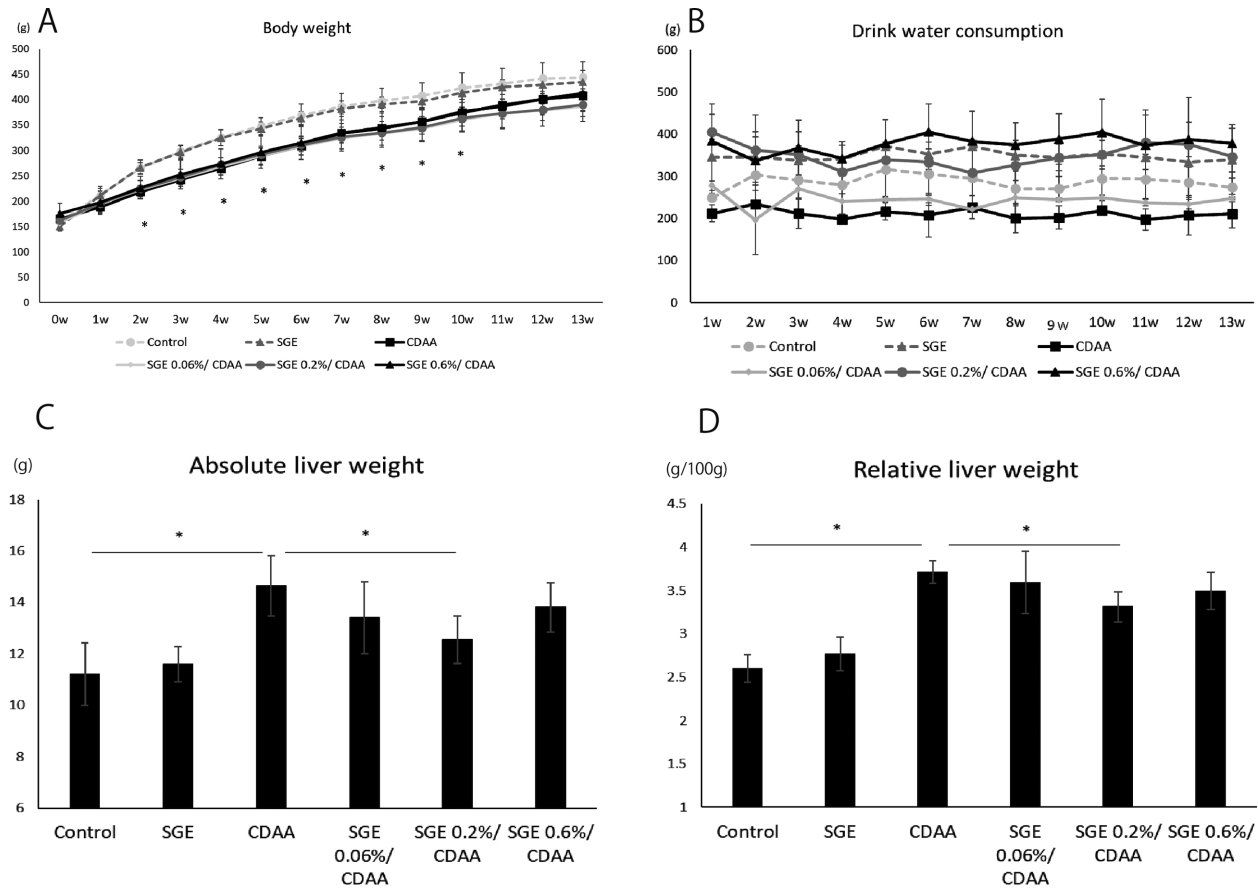


Fig. 1. Changes in DPPH radical scavenging activities. (A) Absorbances measured at 520 nm and (B) radical scavenging activity. DPPH: 1,1-diphenyl-2-picrylhydrazyl; SGE: *Siraitia grosvenorii* extract.

The CDAA diet could induce oxidative stress, as indicated by hepatic Gpx2 mRNA levels and activation of NF- $\kappa$ B. *S. grosvenerii* has been shown to suppress oxidative stress *in vivo*<sup>14</sup>. Similarly, the CDAA diet could induce

hepatotoxicity, as indicated by serum AST and ALT levels, upregulation of hepatic Mcp-1 mRNA, and CD68 immuno-histochemical positive staining. Based on TUNEL staining, the CDAA diet induced hepatocyte apoptosis. Moreover,



**Fig. 2.** Changes in drinking water intake, body weight, and liver weight. (A) Changes in drinking water intake, (B) body weight, (C) absolute liver weight, and (D) relative liver weight during the experiment. Data are presented as mean  $\pm$  standard deviation. \*Significantly different ( $p < 0.05$ ). SGE: *Siraitia grosvenerii* extract; CDAA: choline-deficient, methionine-lowered, L-amino acid-defined.

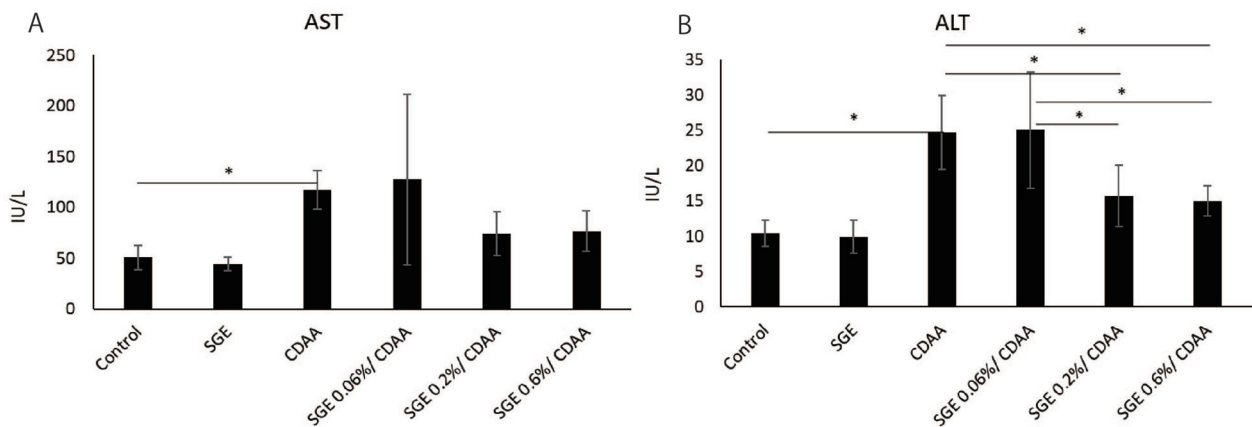


**Fig. 3.** Changes in serum activities of (A) AST and (B) ALT. Data are presented as mean  $\pm$  standard deviation. \*Significantly different ( $p < 0.05$ ). ALT: alanine aminotransferase; AST: aspartate aminotransferase; SGE: *Siraitia grosvenerii* extract; CDAA: choline-deficient, methionine-lowered, L-amino acid-defined.

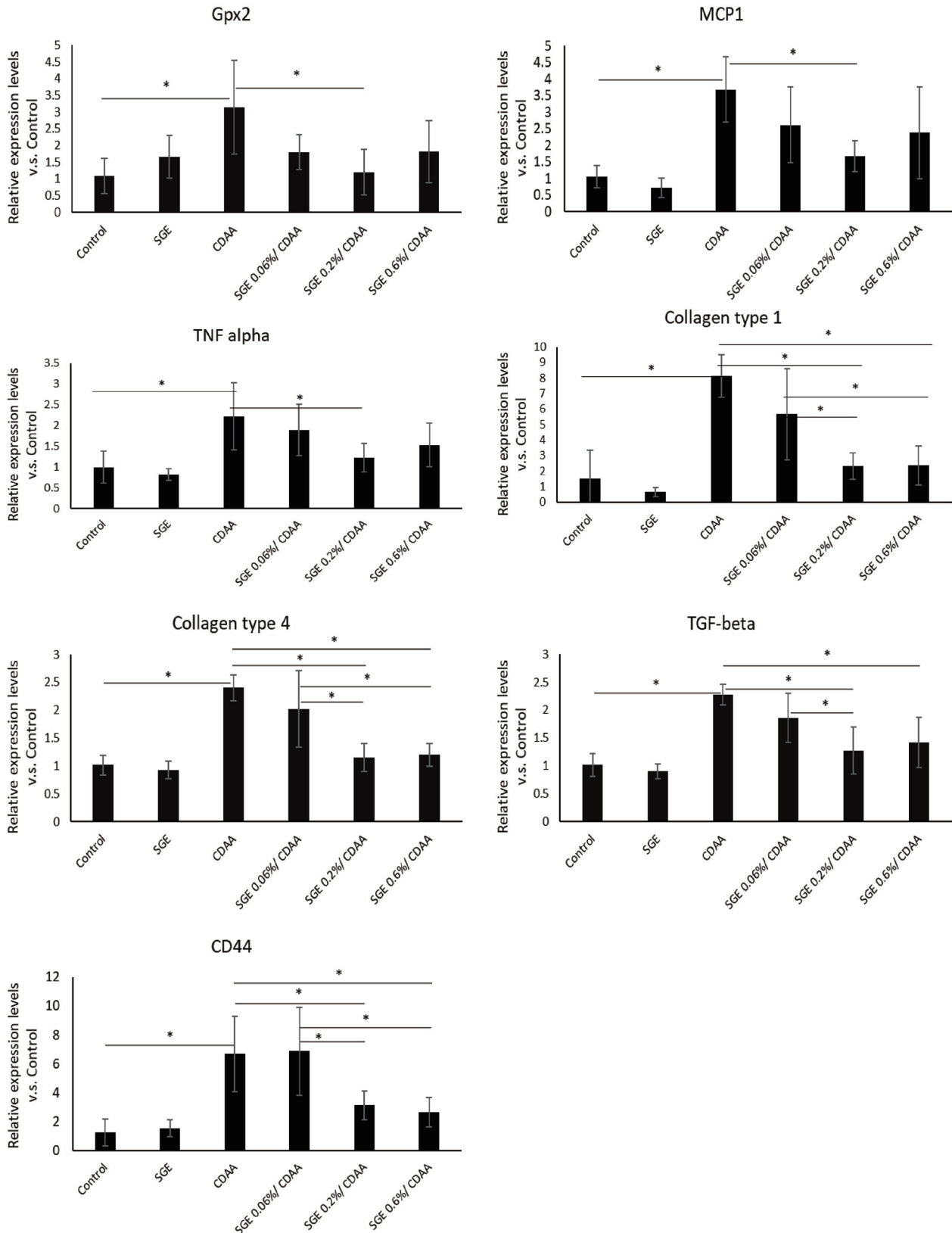


**Fig. 4.** Changes in hepatic gene expression. Changes in hepatic mRNA expression of *Gpx-2*, *Mcp-1*, *TNF-alpha*, *collagen type 1*, *collagen type 4*, *Tgf $\beta$* , and *CD44*. Data are presented as mean  $\pm$  standard deviation. \*Significantly different ( $p < 0.05$ ). SGE: *Siraitia grosvenorii* extract; CDAA: choline-deficient, methionine-lowered, L-amino acid-defined.

the CDAA diet increased the number of CD44-positive bile duct cells and promoted hepatic fibrosis, as indicated by the histopathological and gene expression analyses. SGE administration could ameliorate these changes, especially at

0.2% SGE. The efficacy of 0.6% SGE was lower than that of 0.2% SGE; however, no apparent toxicity was observed. In contrast, no clear effect was detected with 0.06% SGE, and some results suggested disease progression. These results indicate the optimal concentration of SGE under these conditions.

Some of the mitigating effects of SGE on NASH lesions could be attributed to a specific antioxidant. Suppression of oxidative stress can be associated with decreased inflammation and fibrosis in the liver<sup>18</sup>. Furthermore, mogrosin V, a biologically active substance in SGE, significantly reduced the expression of pro-inflammatory cytokines in lipopolysaccharide-stimulated macrophages *in vitro*<sup>19</sup>. Similarly, in the present study, we predicted that these effects would contribute to alleviating CDAA diet-induced diseases.

In addition, the findings of the present study suggest that CD44 is a key factor controlling NASH lesions, consistent with the findings of previous studies demonstrating that CD44 specifically controls inflammation and fibrosis<sup>20, 21</sup>. CD44 contributes to the progression of NASH lesions via infiltration and polarization of macrophages<sup>20</sup>. Moreover, the appearance of positive cells in the bile duct contributes to hyaluronic acid deposition and the promotion of liver fibrosis<sup>21</sup>. Herein, CD44 was significantly suppressed following SGE administration at concentrations exceeding 0.2%; the expression of hepatic mRNA and immunohistopathological positive cells were reduced in the intrahepatic bile duct. CD44 is a major hyaluronan receptor, and its binding is enhanced during hepatic inflammation and fibrosis<sup>22</sup>. Under the CDAA diet, hyaluronan was deposited in the surrounding CD44-positive cells in the bile ducts, which progressed to hepatic fibrosis. However, SGE also suppressed fibrosis by downregulating CD44 expression.

The phosphorylation of NF-κB was increased in the CDAA diet-fed groups. NF-κB is regulated by various fac-

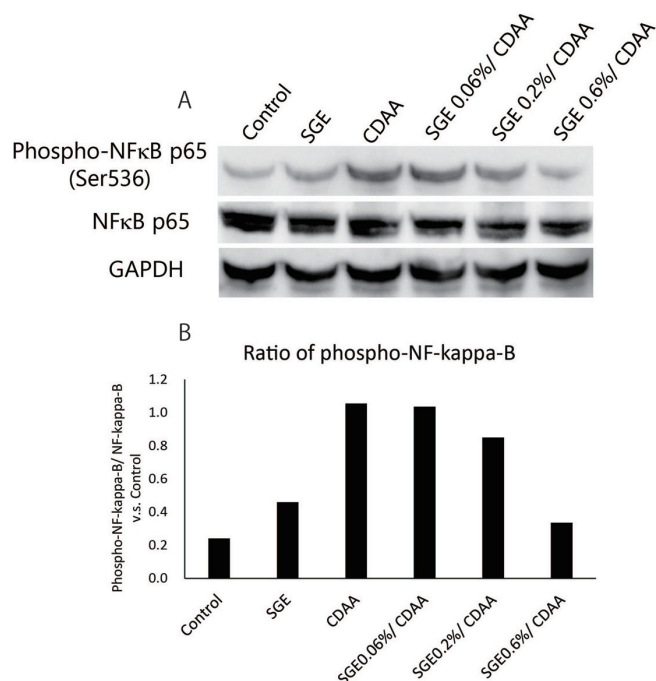


**Fig. 5.** Western blotting analysis. Comparison of expression levels of NF-kappa-B and phospho-NF-kappa-B between groups. (A) Western blotting analysis. (B) The ratio of phospho-NF-kappa-B/NF-kappa-B. Data are presented as mean ± standard deviation. \*Significantly different ( $p < 0.05$ ). SGE: *Siraitia grosvenorii* extract; CDAA: choline-deficient, methionine-lowered, L-amino acid-defined.

**Table 4.** CD68-positive Macrophage Infiltration Score

Finding	Animal	Control						SGE						CDAA					
	Animal No.	1	2	3	4	5	6	7	8	9	10	11	12	13	14	15	16	17	18
Liver																			
Infiltration, CD68-positive macrophage		±	±	±	±	±	±	±	±	±	±	±	±	±	±	±	±	±	±
Finding		SGE 0.06%/ CDAA						SGE 0.02%/ CDAA						SGE 0.6%/ CDAA					
Animal No.		19	20	21	22	23	24	25	26	27	28	29	30	31	32	33	34	35	36
Liver																			
Infiltration, CD68-positive macrophage		2+	2+	2+	+	2+	2+	+	+	2+	2+	+	2+	2+	+	+	2+	2+	2+

– : Negative, ± : Very slight, + : Slight, 2+ : Moderate, 3+ : Severe.

SGE: *Siraitia grosvenorii* extract; CDAA: choline-deficient, methionine-lowered, L-amino acid.

**Table 5.** Number and Area of Glutathione-S-transferase Placental Form (GST-P) Foci

GST-P	CDAA	SGE 0.06%/ CDAA	SGE 0.2%/ CDAA	SGE 0.6%/ CDAA
Number (foci/ sample)	1	4	2	1
foci area/ section area	0.0022%	0.0149%	0.0004%	0.0012%

SGE: *Siraitia grosvenorii* extract; CDAA: choline-deficient, methionine-lowered, L-amino acid.

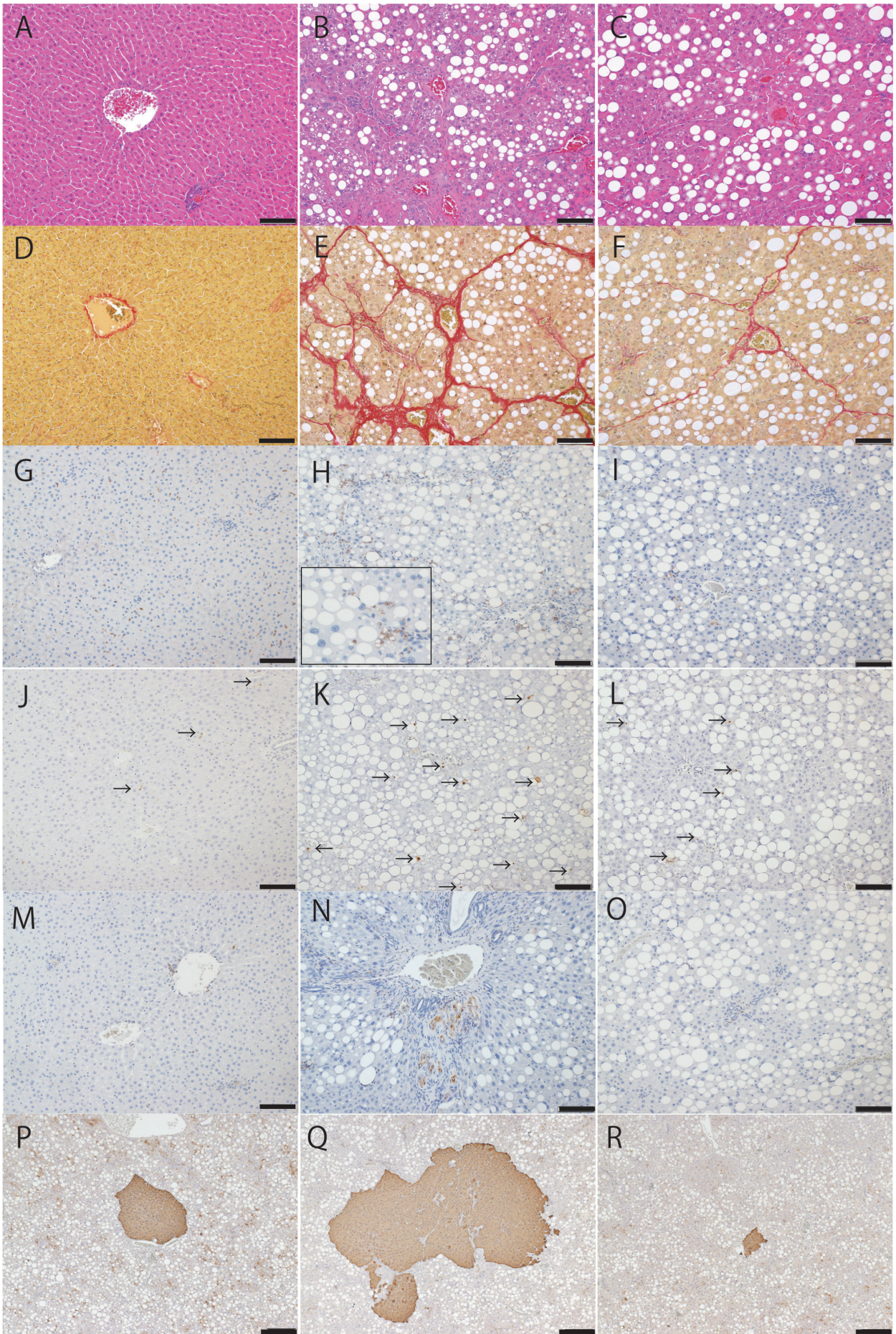
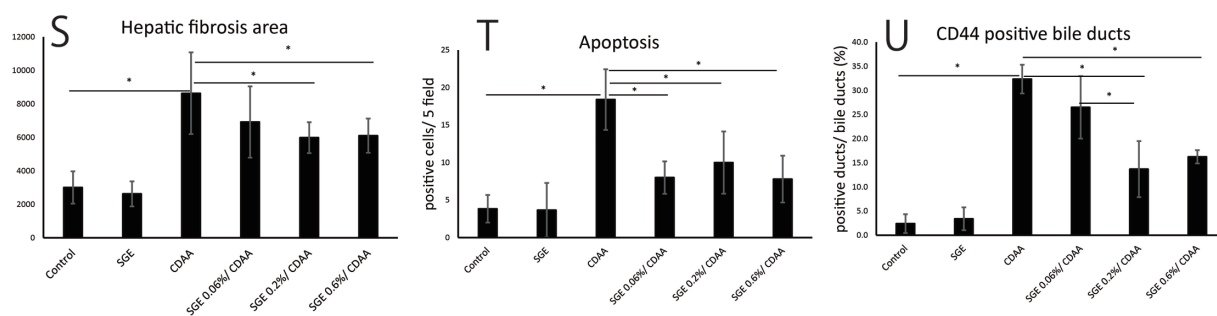


Fig. 6.



**Fig. 6.** Morphological changes in the liver. (A) Representative outcomes in the liver examined by hematoxylin-eosin (H&E) staining of control, (B) CDAA, and (C) SGE 0.2%/CDAA. (D) Representative Sirius Red (SR) staining of control, (E) CDAA and (F) SGE 0.2%/CDAA. (G) Representative CD68 immunohistochemistry of control, (H) CDAA, and (I) SGE 0.2%/CDAA. (J) Representative TUNEL staining of control, (K) CDAA, and (L) SGE 0.2%/CDAA. The black arrow indicates apoptotic cells. (M) Representative CD44 immunohistochemistry of control, (N) CDAA, and (O) SGE 0.2%/CDAA. (P) Representative GST-P immunohistochemistry of the positive foci in CDAA and (Q) positive foci in SGE 0.06%/CDAA, and (R) SGE 0.2%/CDAA. (S) The SR-stained fibrotic area, (T) the TUNEL-stained number of apoptotic cells per 5 fields, and (U) CD44-positive bile duct percentage in CD44 liver immunohistochemistry. Data are presented as mean  $\pm$  standard deviation. \*Significantly different ( $p < 0.05$ ). Black scale bar: 100  $\mu$ m; white bar: 200  $\mu$ m. CDAA: choline-deficient, methionine-lowered, L-amino acid; SGE: *Siraitia grosvenorii* extract.

tors such as TNF- $\alpha$ , interleukin-1  $\beta$ , and oxidative stress<sup>23</sup>. Phosphorylation of activated NF- $\kappa$ B regulates the expression of CD44<sup>24,25</sup>. Furthermore, interactions between CD44 and hyaluronan are reportedly mediated by NF- $\kappa$ B activation via PI3K and AKT<sup>26</sup>. In the present study, CD44 expression, as determined by histopathological and gene expression analyses, was similar to the changes in NF- $\kappa$ B activation. Our findings suggest that SGE-induced effects could be attributed to the modulation of CD44 expression via NF- $\kappa$ B. Thus, the antioxidative effects of SGE are, at least partly, attributed to these inhibitors including NF- $\kappa$ B.

Taken together, SGE at concentrations  $>0.2\%$  in drinking water did not induce toxicity and decreased oxidative stress, apoptosis, inflammation, precancerous lesions, and fibrosis in the CDAA diet-induced liver. These results were mediated via the regulation of CD44 expression via NF- $\kappa$ B, thereby indicating the antioxidative effect of SGE. SGE may be useful for controlling lifestyle diseases, such as NASH, by suppressing oxidative stress. Detailed analysis of oxidative stress and CD44 in NASH and the effect of SGE may lead to the identification of new therapeutic targets in NASH and liver fibrosis.

**Disclosure of Potential Conflicts of Interest:** In the present study, SGE was supplied by San-Ei Gen F.F.I., but the study was conducted independently of the company.

**Acknowledgments:** We thank the members of our laboratories, particularly Dr. Shim-mo Hayashi (National Institute of Health Sciences), Ms. Mihoko Koyanagi (San-Ei Gen F.F.I., Inc.), and Ms. Marika Matsumoto (Tokyo University of Agriculture). We also thank the coauthors of this study for their discussions and helpful comments. This study was supported in part by the Tokyo University of Agriculture.

## References

- John OD, du Preez R, Panchal SK, and Brown L. Tropical foods as functional foods for metabolic syndrome. *Food Funct.* **11**: 6946–6960. 2020. [Medline] [CrossRef]
- Kawada T. Food-derived regulatory factors against obesity and metabolic syndrome. *Biosci Biotechnol Biochem.* **82**: 547–553. 2018. [Medline] [CrossRef]
- Brown L, Poudyal H, and Panchal SK. Functional foods as potential therapeutic options for metabolic syndrome. *Obes Rev.* **16**: 914–941. 2015. [Medline] [CrossRef]
- Burt AD, Lackner C, and Tiniakos DG. Diagnosis and assessment of NAFLD: definitions and histopathological classification. *Semin Liver Dis.* **35**: 207–220. 2015. [Medline] [CrossRef]
- Dulai PS, Singh S, Patel J, Soni M, Prokop LJ, Younossi Z, Sebastiani G, Ekstedt M, Hagstrom H, Nasr P, Stal P, Wong VW, Kechagias S, Hulcrantz R, and Loomba R. Increased risk of mortality by fibrosis stage in nonalcoholic fatty liver disease: Systematic review and meta-analysis. *Hepatology.* **65**: 1557–1565. 2017. [Medline] [CrossRef]
- Nakae D. Endogenous liver carcinogenesis in the rat. *Pathol Int.* **49**: 1028–1042. 1999. [Medline] [CrossRef]
- Nakae D, Yoshiji H, Maruyama H, Kinugasa T, Denda A, and Konishi Y. Production of both 8-hydroxydeoxyguanosine in liver DNA and gamma-glutamyltransferase-positive hepatocellular lesions in rats given a choline-deficient, L-amino acid-defined diet. *Jpn J Cancer Res.* **81**: 1081–1084. 1990. [Medline] [CrossRef]
- Van Herck MA, Vonghia L, and Francque SM. Animal models of nonalcoholic fatty liver disease—a starter's guide. *Nutrients.* **9**: 1072. 2017. [Medline] [CrossRef]
- Li C, Lin LM, Sui F, Wang ZM, Huo HR, Dai L, and Jiang TL. Chemistry and pharmacology of *Siraitia grosvenorii*: a review. *Chin J Nat Med.* **12**: 89–102. 2014. [Medline]
- Li H, Li R, Jiang W, and Zhou L. Research progress of pharmacological effects of *Siraitia grosvenorii* extract. *J Pharm Pharmacol.* **74**: 953–960. 2022. [Medline]

11. Zhang X, Song Y, Ding Y, Wang W, Liao L, Zhong J, Sun P, Lei F, Zhang Y, and Xie W. Effects of Mogrosides on high-fat-diet-induced obesity and nonalcoholic fatty liver disease in mice. *Molecules*. **23**: 1894. 2018. [[Medline](#)] [[CrossRef](#)]
12. Li L, Zheng W, Wang C, Qi J, and Li H. Mogroside V protects against hepatic steatosis in mice on a high-fat diet and LO2 cells treated with free fatty acids via AMPK activation. *Evid Based Complement Alternat Med*. **2020**: 7826874. 2020. [[Medline](#)]
13. Suzuki-Kemuriyama N, Abe A, Nakane S, Uno K, Ogawa S, Watanabe A, Sano R, Yuki M, Miyajima K, and Nakae D. Extract of *Siraitia grosvenorii* (Luo Han Guo) protects against hepatic fibrosis in mice on a choline-deficient, methionine-lowered, L-amino acid-defined, high-fat diet without trans fatty acids. *Fundam Toxicol Sci*. **8**: 135–145. 2021. [[CrossRef](#)]
14. Matsumoto S, Jin M, Dewa Y, Nishimura J, Moto M, Murata Y, Shibutani M, and Mitsumori K. Suppressive effect of *Siraitia grosvenorii* extract on dicyclanil-promoted hepatocellular proliferative lesions in male mice. *J Toxicol Sci*. **34**: 109–118. 2009. [[Medline](#)] [[CrossRef](#)]
15. Suzuki YA, Tomoda M, Murata Y, Inui H, Sugiura M, and Nakano Y. Antidiabetic effect of long-term supplementation with *Siraitia grosvenori* on the spontaneously diabetic Goto-Kakizaki rat. *Br J Nutr*. **97**: 770–775. 2007. [[Medline](#)] [[CrossRef](#)]
16. Jin M, Muguruma M, Moto M, Okamura M, Kashida Y, and Mitsumori K. Thirteen-week repeated dose toxicity of *Siraitia grosvenori* extract in Wistar Hannover (GALAS) rats. *Food Chem Toxicol*. **45**: 1231–1237. 2007. [[Medline](#)] [[CrossRef](#)]
17. Gong X, Chen N, Ren K, Jia J, Wei K, Zhang L, Lv Y, Wang J, and Li M. The fruits of *Siraitia grosvenorii*: a review of a Chinese food-medicine. *Front Pharmacol*. **10**: 1400. 2019. [[Medline](#)] [[CrossRef](#)]
18. Li S, Tan HY, Wang N, Zhang ZJ, Lao L, Wong CW, and Feng Y. The role of oxidative stress and antioxidants in liver diseases. *Int J Mol Sci*. **16**: 26087–26124. 2015. [[Medline](#)] [[CrossRef](#)]
19. Zhou Y, Hu Z, Ye F, Guo T, Luo Y, Zhou W, Qin D, Tang Y, Cao F, Luo F, and Lin Q. Mogroside V exerts anti-inflammatory effect via MAPK-NF- $\kappa$ B/AP-1 and AMPK-PI3K/Akt/mTOR pathways in ulcerative colitis. *J Funct Foods*. **87**: 104807. 2021. [[CrossRef](#)]
20. Patouraux S, Rousseau D, Bonnafous S, Lebeaupin C, Luci C, Canivet CM, Schneck AS, Bertola A, Saint-Paul MC, Iannelli A, Gugenheim J, Anty R, Tran A, Bailly-Maitre B, and Gual P. CD44 is a key player in non-alcoholic steatohepatitis. *J Hepatol*. **67**: 328–338. 2017. [[Medline](#)] [[CrossRef](#)]
21. Uno K, Miyajima K, Toma M, Suzuki-Kemuriyama N, and Nakae D. CD44 expression in the bile duct epithelium is related to hepatic fibrosis in nonalcoholic steatohepatitis rats induced by a choline-deficient, methionine-lowered, L-amino acid diet. *J Toxicol Pathol*. **35**: 149–157. 2022. [[Medline](#)] [[CrossRef](#)]
22. Li Y, Jiang D, Liang J, Meltzer EB, Gray A, Miura R, Wogenshen L, Yamaguchi Y, and Noble PW. Severe lung fibrosis requires an invasive fibroblast phenotype regulated by hyaluronan and CD44. *J Exp Med*. **208**: 1459–1471. 2011. [[Medline](#)] [[CrossRef](#)]
23. Nakanishi C, and Toi M. Nuclear factor-kappaB inhibitors as sensitizers to anticancer drugs. *Nat Rev Cancer*. **5**: 297–309. 2005. [[Medline](#)] [[CrossRef](#)]
24. Smith SM, and Cai L. Cell specific CD44 expression in breast cancer requires the interaction of AP-1 and NF $\kappa$ B with a novel cis-element. *PLoS One*. **7**: e50867. 2012. [[Medline](#)] [[CrossRef](#)]
25. Smith SM, Lyu YL, and Cai L. NF- $\kappa$ B affects proliferation and invasiveness of breast cancer cells by regulating CD44 expression. *PLoS One*. **9**: e106966. 2014. [[Medline](#)] [[CrossRef](#)]
26. Jordan AR, Racine RR, Hennig MJ, and Lokeshwar VB. The role of CD44 in disease pathophysiology and targeted treatment. *Front Immunol*. **6**: 182. 2015. [[Medline](#)] [[CrossRef](#)]